Supplementary information for *A first-principles description of proton-driven spin diffusion*

Jean-Nicolas Dumez, Meghan E. Halse, Mark C. Butler, and Lyndon Emsley

A. Identification of the "relevant" constants of motion

The evolution of any system under the influence of a Liouvillian, L, can be characterized by a set of constants of motion $\{A_n\}$, defined as the eigenoperators of L that correspond to eigenvalues of zero. The "relevant" constants of motion are those that contribute to the observables of interest, e.g. the single-spin polarizations $\{S_z\}$. One case of particular interest to this Communication is that in which the only relevant constant of motion is the total polarization, $F_z = \sum_{j=1}^{N} S_{jz}$. The existence of the total polarization as the only relevant constant of motion is a property that can be identified in full or reduced Liouville space simulations using the following numerical procedure.

1. Build an explicit representation of the Liouvillian, such that the spin-space reduction (if desired) can be achieved through an appropriate truncation of the full Liouvillian.

2. For the case of samples undergoing magic-angle spinning, calculate the average propagator over a single rotor period by assuming a step-wise time-independent interaction.

3. Diagonalize the average propagator to obtain an effective Liouvillian and the associated eigenoperators. (In the case of a static sample, diagonalize the static Liouvillian to obtain the eigenoperators and eigenvalues directly.)

4. Extract the constants of motion of the system from the complete set of eigenoperators through identification of the eigenvalues of the effective Liouvillian that are equal to zero.

5. Identify the contribution of the single-spin polarizations to the constants of motion by visual inspection. If the contributions of the single-spin polarizations to each constant of motion are equal (i.e. $\langle S_{iz}|A_n\rangle = \langle S_{jz}|A_n\rangle$ for all i, j and n,) the total polarization is the only relevant constant of motion.

The above procedure was applied to a large number of spin-diffusion simulations of medium-sized systems (≤ 8 spins) of both homonuclei (the PSD case) and heteronuclei (the PDSD case) with a variety of coupling constants, MAS rates and spin-space reduction schemes. It was found that the total polarization was the only relevant constant of motion for all LCL simulations of spin diffusion regardless of (i) MAS rate, (ii) the extent of spin-space reduction and (iii) the size of the spin system, the notable exceptions being simulations of static samples ($\omega_r = 0$), simulations of very small spin systems ($N < 5$) and full-space simulations ($q_{\max} = N$).

B. Comparing experimental and simulated PDSD build-up curves

1. Experimental

Proton-driven spin diffusion can be observed experimentally using the 2D pulse sequence in Fig. 1 for a set of mixing times $\{\tau\}$. In the 2D spectrum a transfer of polarisation during the mixing time τ from spins observed at frequency ν_1 to spins observed at frequency ν_2 results in a cross peak at frequency coordinates (ν_1, ν_2). The peak volumes as a function of the mixing time τ, $P_{exp}(\nu_1, \nu_2, \tau)$, can be conveniently arranged in a $M \times M$ matrix, where

M is the number of resolved peaks in the 1D spectrum, and are usually plotted as a $M \times M$ matrix of build-up curves.
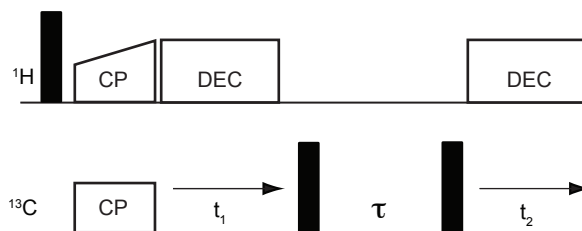

FIG. 1: Pulse sequence for the 2D PDSD experiment.

Experimental proton-driven spin diffusion data have been recorded for L-histidine.H_2O.HCl at MAS frequencies of 10, 15 and 20 kHz and at a ^{1}H Larmor frequency of 700 MHz; the experimental details have been reported previously.[1]

2. Simulated

The volume of the (ν_1, ν_2) peak for a mixing time τ can be written formally:

$$P_{sim}(\nu_1, \nu_2, \tau) = \langle \sum_{j=1}^{N_2} I_{b_j z} | \hat{U}(\tau) | \sum_{i=1}^{N_1} I_{a_i z} \rangle, \qquad (1)$$

where the first and second summations are over groups of spins $\{a_i\}_{i=1,N_1}$ and $\{b_j\}_{j=1,N_2}$ that are observed at frequency ν_1 and ν_2, respectively and $\hat{U}(\tau)$ is the time-evolution super-operator for a mixing time τ. For simulations of polarisation transfer among six spins with resolved resonances, the expression for the peak volume can be simplified to:

$$P_{sim}(\nu_1, \nu_2, \tau) = \langle I_{b_1 z} | \hat{U}(\tau) | I_{a_1 z} \rangle, \qquad (2)$$

where a_1 is the spin observed at frequency ν_1 and b_1 is the spin observed at frequency ν_2. Consequently, the build-up curves are simulated by performing one independent calculation for each spin in the system, with an initial density matrix that corresponds to a single polarised spin $\sigma(0) = I_{a_1 z}$, and observables that consist of all the single-spin polarisations.

For the systems studied here, proton positions were taken from single crystal X-ray diffraction data available from the Cambridge Structural Database (entry code HISTCM12). Each simulation, for a given orientation and a given initial density matrix, took 20 h on a 2.83 GHz processor and required 90 MB of memory.

3. Comparison

The experimental and simulated spin diffusion build-up curves are related by an overall normalisation factor

$$P_{exp}(\nu_1, \nu_2, \tau) = \xi P_{sim}(\nu_1, \nu_2, \tau), \qquad (3)$$

where ξ depends on many experimental contributions that are not measured. In order to compare simulated and experimental data, ξ is determined from a least-squares fit between

the calculated and experimental peak volumes. Separate values are obtained for each initial density matrix, i.e., for each line in the $M \times M$ matrix of build-up curves; these additional degrees of freedom make it possible to account for some effects that are not included in the simulation, such as the efficiency of the cross-polarisation step.

C.   Additional PDSD build-up curves

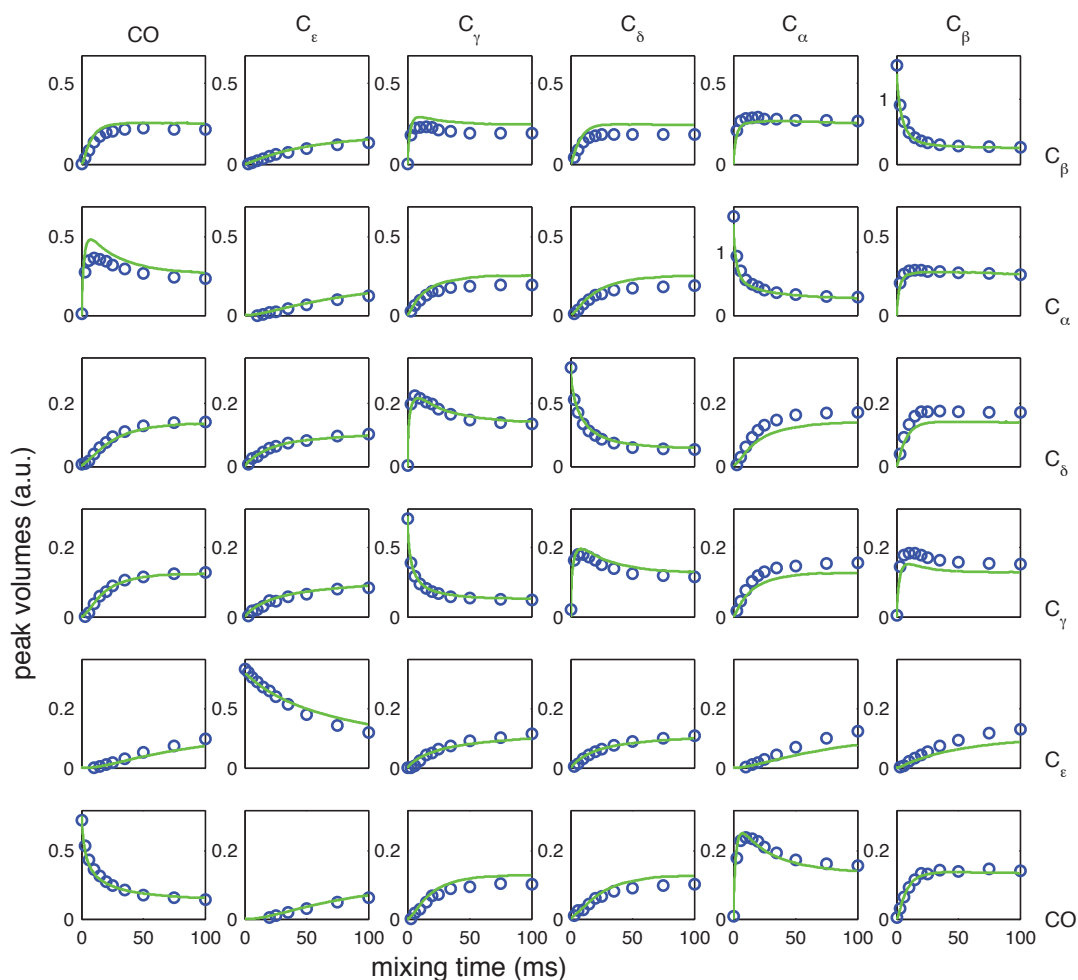[1] J.-N. Dumez and L. Emsley, Phys. Chem. Chem. Phys. **13**, 7363 (2011).
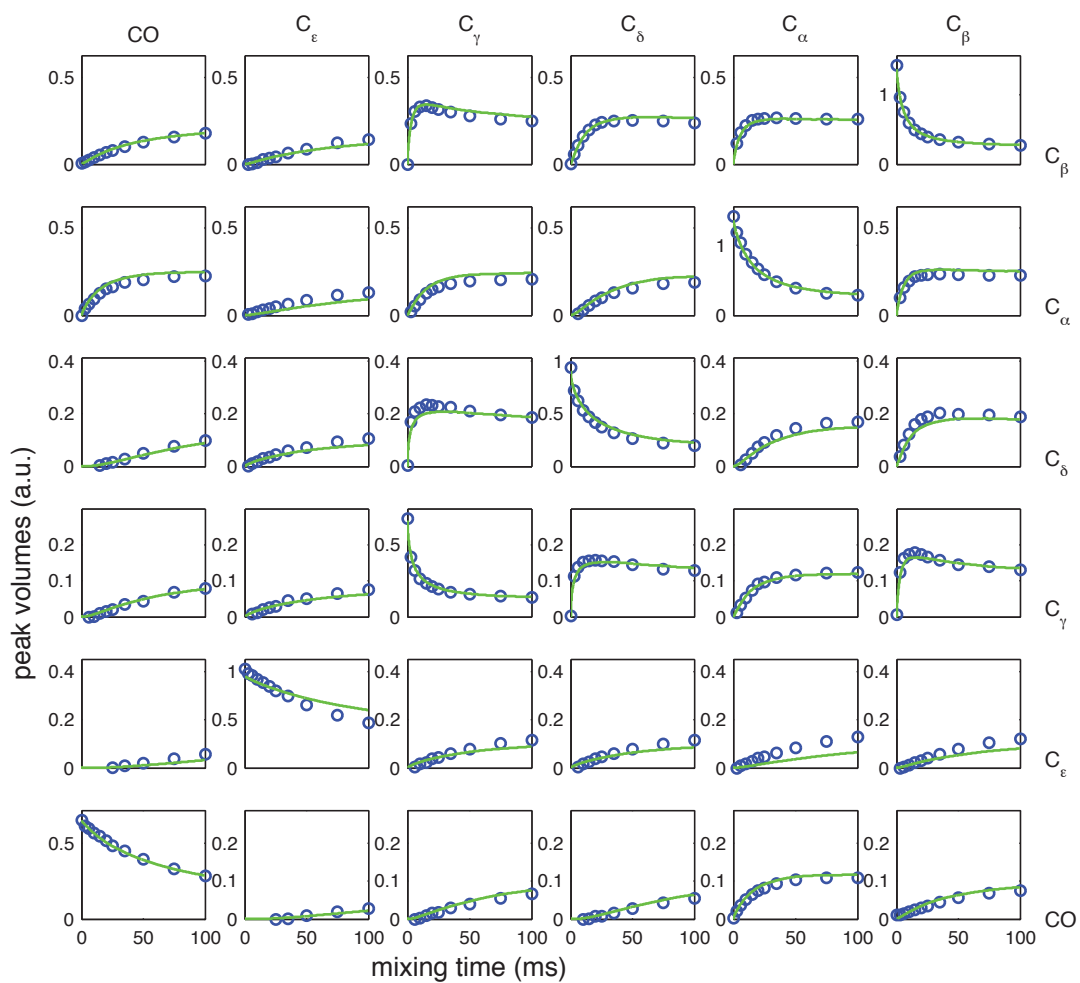
FIG. 2: Comparison between experimental (blue) and simulated (green) proton driven spin diffusion build-up curves for a powdered sample of L-histidine.H_2O.HCl under 10 kHz MAS. The simulated curves were obtained from LCL simulations of a system of 6 carbons and 10 protons, consisting of a single molecule of L-histidine.H_2O.HCl. Atomic coordinates are taken from a crystal structure (CSD entry: histcm12). The time step in the simulation is 0.5 μs, and a ZCW set of 50 orientations is used for the powder average.
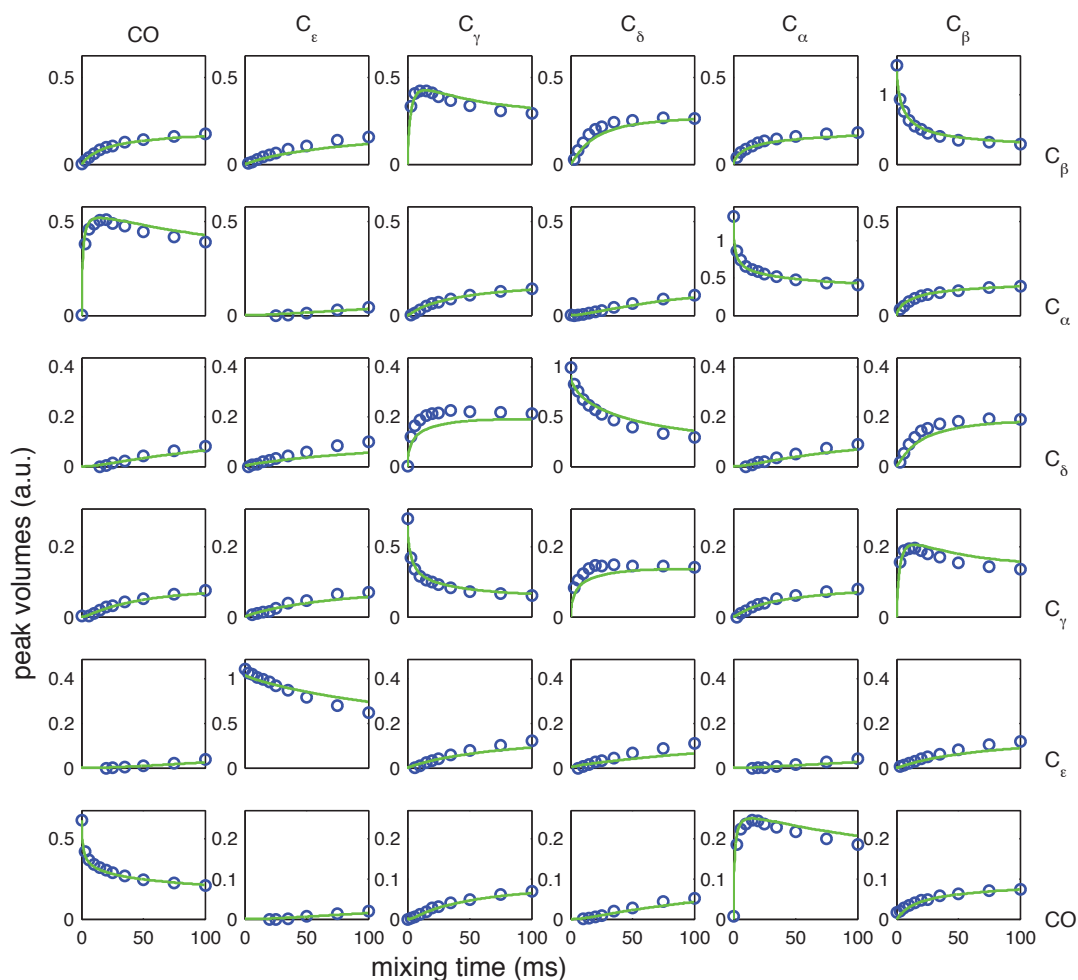
5

FIG. 3: Comparison between experimental (blue) and simulated (green) proton driven spin diffusion build-up curves for a powdered sample of L-histidine.H$_2$O.HCl under 15 kHz MAS. The simulated curves were obtained from LCL simulations of a system of 6 carbons and 10 protons, consisting of a single molecule of L-histidine.H$_2$O.HCl. The atomic coordinates, timestep and set of orientations are the same as in Fig. 2.

FIG. 4: Comparison between experimental (blue) and simulated (green) proton driven spin diffusion build-up curves for a powdered sample of L-histidine.H_2O.HCl under 20 kHz MAS. The simulated curves were obtained from LCL simulations of a system of 6 carbons and 10 protons, consisting of a single molecule of L-histidine.H_2O.HCl. The atomic coordinates, timestep and set of orientations are the same as in Fig. 2.
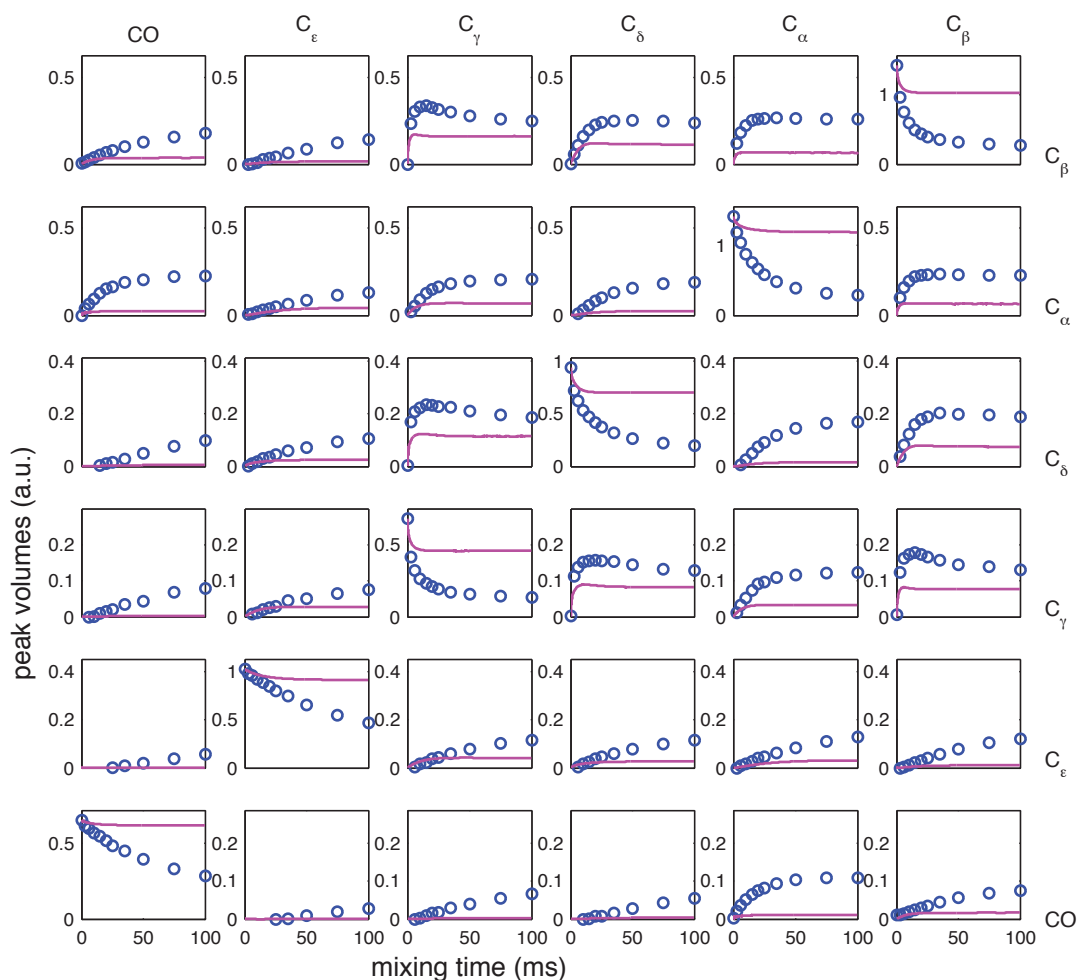
FIG. 5: Comparison between experimental (blue) and simulated (magenta) proton-driven spin diffusion build-up curves for a powdered sample of L-histidine.H$_2$O.HCl under 15 kHz MAS. The simulated curves were obtained from full-space simulations of a system of 6 carbons and 7 protons, consisting of all the carbons of a molecule of L-histidine.H$_2$O.HCl and of the 7 protons that are the most strongly coupled to these carbons. Atomic coordinates are taken from a crystal structure (CSD entry: histcm12), and a ZCW set of 50 orientations is used for the powder average. Here the normalisation for each row was performed so that the calculated and experimental initial volumes of the diagonal peaks are identical.
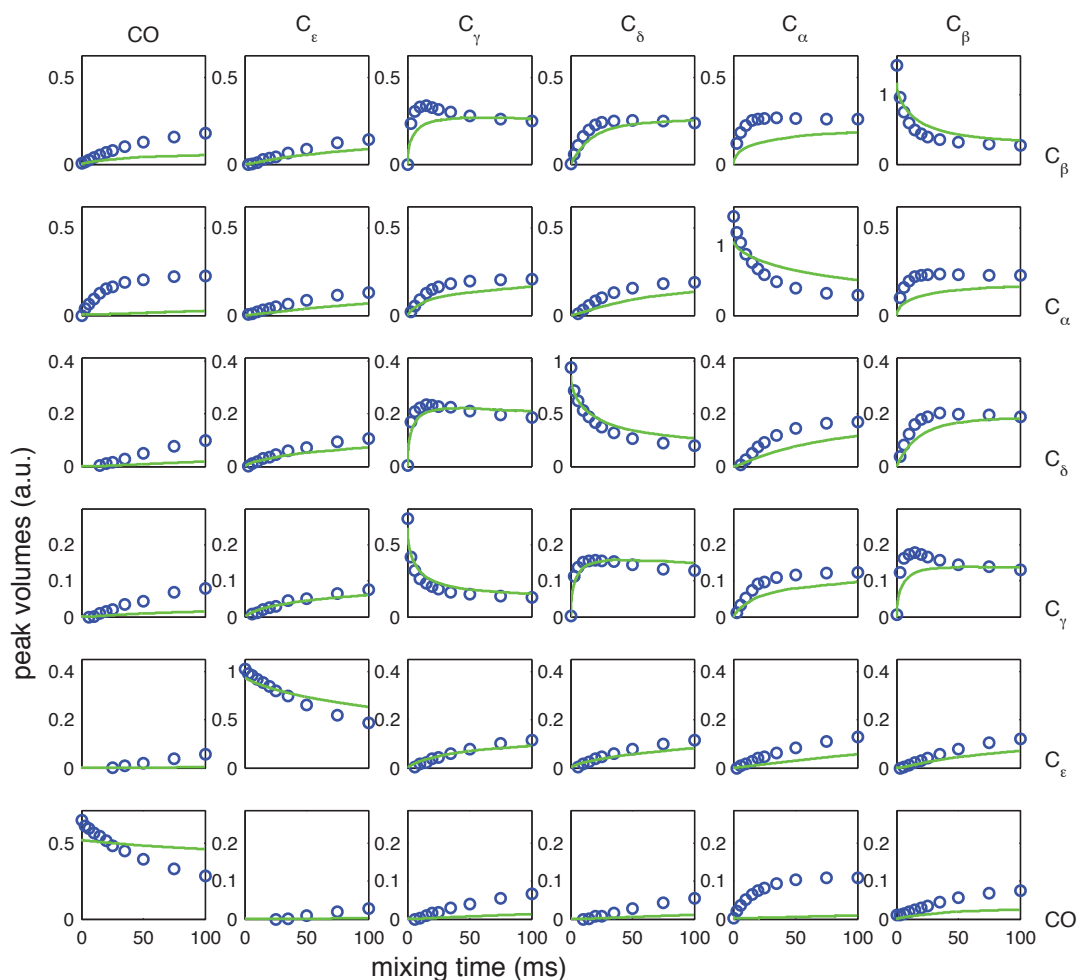
FIG. 6: Comparison between experimental (blue) and simulated (green) proton driven spin diffusion build-up curves for a powdered sample of L-histidine.H₂O.HCl under 15 kHz MAS. The simulated curves were obtained from LCL simulations of a system of 6 carbons and 7 protons, consisting of all the carbons of a molecule of L-histidine.H₂O.HCl and of the 7 protons that are the most strongly coupled to these carbons.. The atomic coordinates, timestep and set of orientations are the same as in Fig. 2.
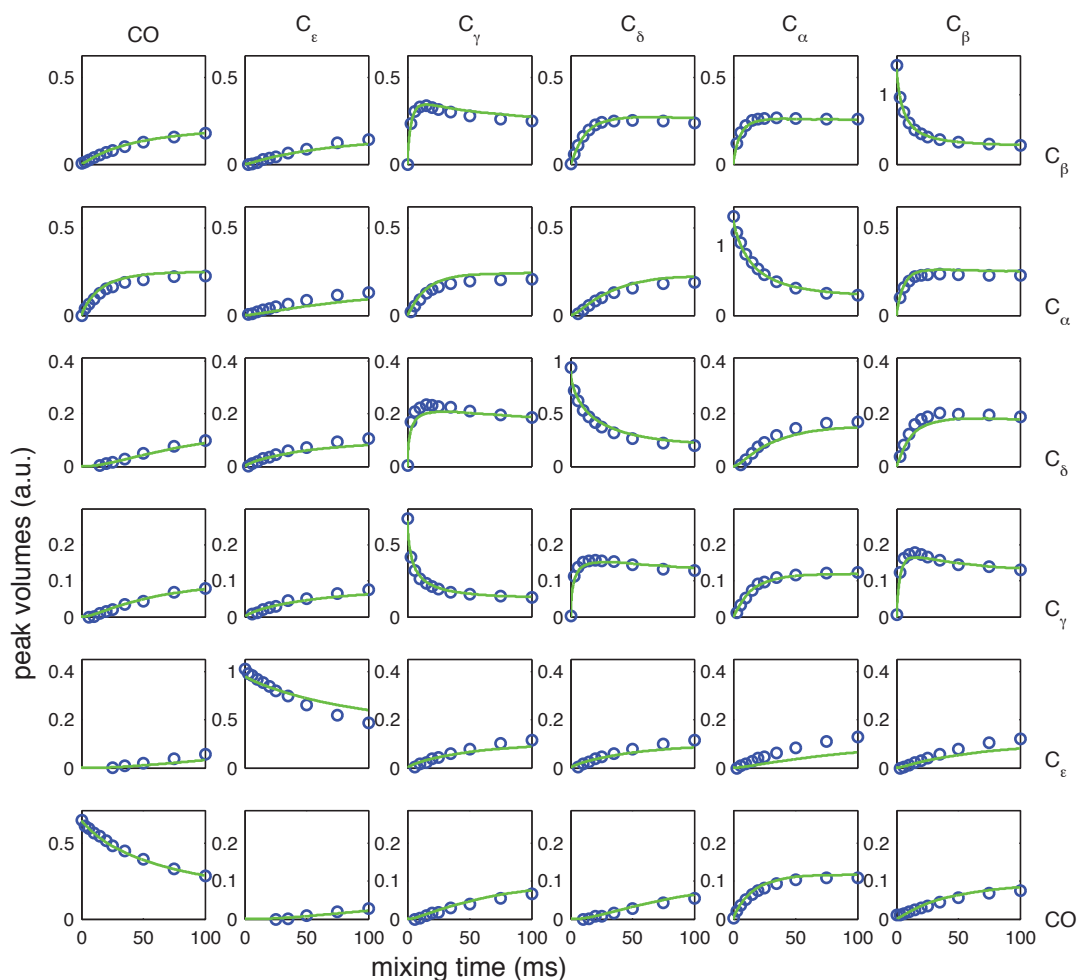
FIG. 7: Comparison between experimental (blue) and simulated (green) proton driven spin diffusion build-up curves for a powdered sample of L-histidine.H_2O.HCl under 15 kHz MAS. The simulated curves were obtained from LCL simulations of a system of 6 carbons and 10 protons, consisting of all the carbons of a molecule of L-histidine.H_2O.HCl and of the 10 protons that are the most strongly coupled to these carbons, i.e., consisting of a single molecule of L-histidine.H_2O.HCl. The atomic coordinates, timestep and set of orientations are the same as in Fig. 2.
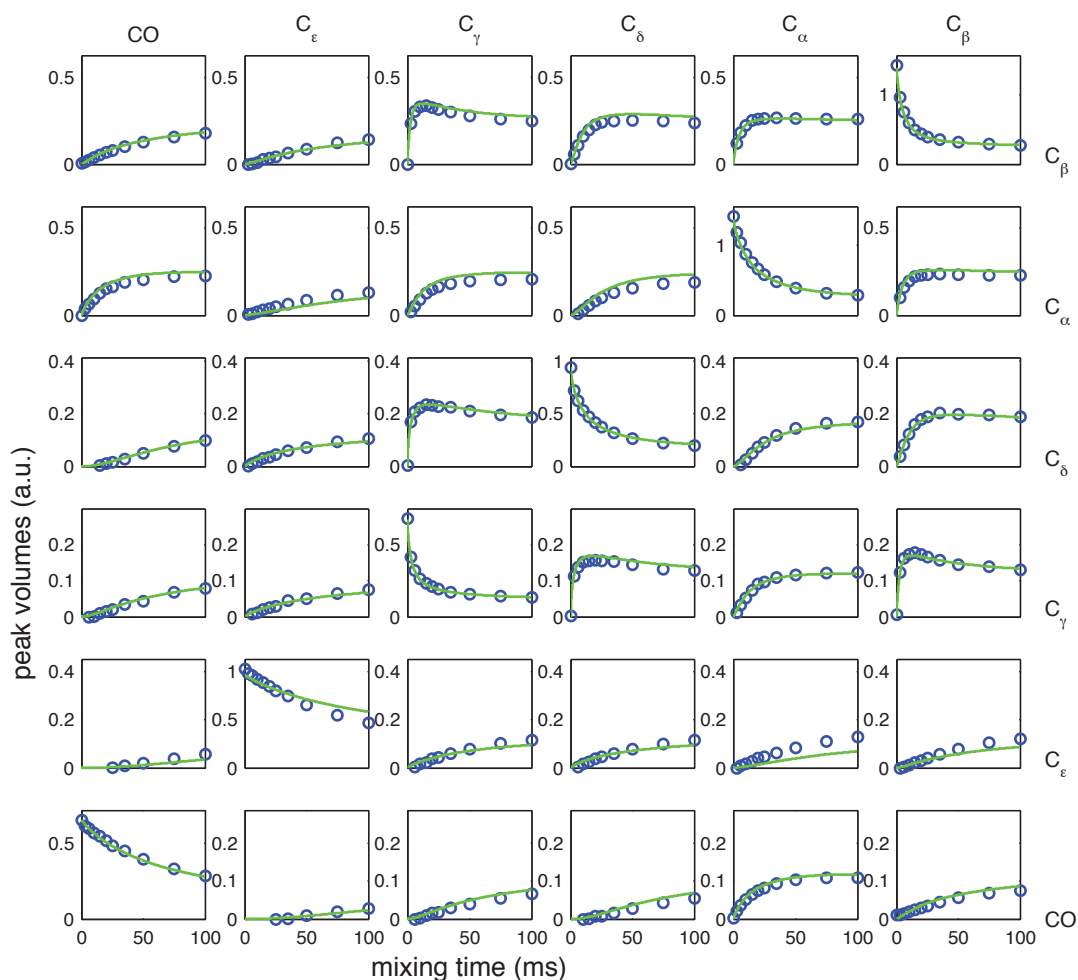
FIG. 8: Comparison between experimental (blue) and simulated (green) proton driven spin diffusion build-up curves for a powdered sample of L-histidine.H$_2$O.HCl under 15 kHz MAS. The simulated curves were obtained from LCL simulations of a system of 6 carbons and 13 protons, consisting of all the carbons of a molecule of L-histidine.H$_2$O.HCl and of the 13 protons that are the most strongly coupled to these carbons. The atomic coordinates, timestep and set of orientations are the same as in Fig. 2.